

Causal drivers of dynamic networks

Melania Lembo^{a*}, Ester Riccardi^{b†}, Veronica Vinciotti^{b‡}, Ernst C. Wit^{a§}

a. Institute of Computing, Università della Svizzera italiana

b. Department of Mathematics, University of Trento

Abstract

Dynamic networks models describe temporal interactions between social actors, and as such have been used to describe financial fraudulent transactions, dispersion of destructive invasive species across the globe, and the spread of fake news. An important question in all of these examples is what are the causal drivers underlying these processes. Current network models are exclusively descriptive and based on correlative structures.

In this paper we propose a causal extension of dynamic network modelling. In particular, we prove that the causal model satisfies a set of population conditions that uniquely identifies the causal drivers. The empirical analogue of these conditions provide a consistent causal discovery algorithm, which distinguishes it from other inferential approaches. Crucially, data from a single environment is sufficient. We apply the method in an analysis of bike sharing data in Washington D.C. in July 2023.

1 Introduction

In this manuscript, our aim is to define a causal dynamic network by means of a structural relational event model. Relational event models were first introduced in Butts (2008) to study instantaneous interactions. Relational events are defined as discrete events in which a sender initiates an interactions directed towards one or more receivers. Bianchi et al. (2024) provide an extensive overview of the developments over the past 15 years of these type of dynamic network models.

Causal discovery aims to find causal relationships between two or more variables, trying to identify which variables affect the outcome. Significant progress has been made in this area over the past 30 years. Indeed, several techniques for detecting causal drivers of a target variable have been developed. First described in Spirtes and Glymour (1991), the PC algorithm aims to identify the Markov equivalence class of the true causal graph

*Corresponding author: melania.lembo@usi.ch.

†ester.ricc@gmail.com

‡veronica.vinciotti@unitn.it

§ernst.jan.camiel.wit@usi.ch

using only conditional independence tests. The PC algorithm comes with some drawbacks. First of all, the complexity increases exponentially with the number of nodes of the graph. Secondly, it is not always possible to define the orientation of all the edges. Indeed, the result is a large class of equivalent DAGs.

The instrumental variable (IV) method identifies the causal structure of a target of interest via an endogenous variable and some conditional independence assumptions associated with this variable (Angrist et al., 1996). It aims to resolve the problem of the presence of unobserved confounders that may affect both the treatment and the outcome.

Recently, new ideas of causal discovery have been suggested that exploit the property of a causal model to be invariant under intervention on variables other than the target one. Peters et al. (2016) show that in a linear Structural Equation Model (SEM) with no confounders invariant causal prediction holds, meaning that under any arbitrary distribution assigned to the covariates X both the linear predictor and the distribution of the additive noise of the target Y are constant. Unfortunately, this method requires that data must be accessible across a number of sufficiently different environments. Furthermore, the procedure is computationally expensive, since it involves a large number of independence statistical tests to identify the causal model. Rothenhäusler et al. (2019) build forth on the invariance idea, by proposing a strategy based on inner-product invariance of the causal residual and the covariates. In principle, observations from the observational environment together with data from a sufficiently richly perturbed environment is sufficient to make the causal model identifiable.

In this paper we will consider a dynamic network $N = \{N_{sr}(t) \mid N_{sr}(t) \in \mathbb{N}_0\}$ and a multivariate covariate process $\mathbf{X} = \{X_{sr}(t) \mid X_{sr}(t) \in \mathbb{R}^p\}$, where the subscripts (s, r) refer to the directed edges of the network. The main question we are interested in answering is which of the covariates \mathbf{X} causally affect the dynamic network N . We will define (X, N) as a structural equation model. Using ideas from invariant causal prediction and focusing on a target variable of interest N , its causal parents X_{PA} affect its distribution and therefore satisfy certain invariance properties, whereas its causal children X_{CH} are consequences of the target itself, which violate these invariance properties. In section 2 we formally define the dynamic network model as a counting process. Under the weak assumption of no simultaneous links, the causal likelihood of the network process can be shown to satisfy a crucial invariance property. Although by itself it is not sufficient to identify the causal model, we show that together the standard MLE property of the causal model, it does identify the causal model uniquely (up to a zero set). In Section 3 we show the performance of the method in a simulation study, whereas in section 4 we illustrate the method by means of a dataset involving bike sharing dynamic network dataset.

2 Causal Dynamic Networks Models

In this section, we define a causal dynamic network model by means of a structural relational event model. This model describes the causal structure of temporal interactions between vertices of a one-mode or two-mode network. The temporal causal structure should not be confused with Granger causality. Instead, the causal nature of the network is defined as a risk invariance under arbitrary perturbations of covariates.

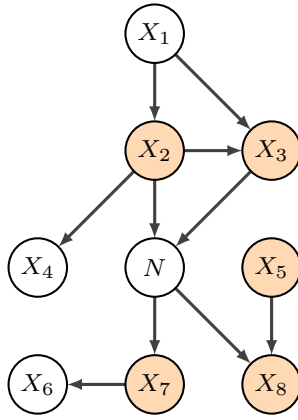


Figure 1: Causal REM with 8 covariates with nodes in orange belonging to the Markov Blanket of the relational process N . The causal parents of N are X_2 and X_3 .

2.1 Structural Relational Event Model

In this section we define the structural relational event model as the joint temporal process of a dynamic network N and a set of potential causal drivers \mathbf{X} on some temporal interval $[0, T]$, i.e., $\{(N(t), \mathbf{X}(t))\}_{t \in [0, T]}$, that satisfies some causal conditions. Let V_1 and V_2 be two sets of vertices. In the case of a one-mode dynamic network, we have that $V_1 \equiv V_2$. A relational event e is defined as a triplet of the type (t, s, r) , where $t \in [0, T]$ is the time of the event connecting, $s \in V_1$ is the sender of the event, and $r \in V_2$ is the receiver. Furthermore, we consider the existence of a marked point process $\mathcal{M} = \{(t_i, (s_i, r_i)) : i \geq 1\}$, in which we assume unique event times t_i and the interactions (s_i, r_i) as marks, as well as a p -dimensional covariate process $\mathbf{X} = \{\mathbf{X}_{sr}(t) \in \mathbb{R}^p \mid t \in [0, T], s \in V_1, r \in V_2\}$. Covariates can be endogenous, when they summarize some part of the dynamic of the network, such as reciprocity. Exogenous covariates are temporal processes that capture other aspects external to the network process, such as the physical distance between the vertices.

We define the structural relational event model as the joint process involving \mathbf{X} and the multivariate counting process $N = \{N_{sr}\}_{(s,r) \in V_1 \times V_2}$, associated with \mathcal{M} that is structurally related to \mathbf{X} . In particular, each component $N_{sr}(t)$ records the number of interactions from s to r that occur until time t . Formally,

$$N_{sr}(t) = \sum_{i \geq 1} \mathbb{1}_{\{t_i \leq t, s_i = s, r_i = r\}},$$

where $N_{sr}(0) = 0$. Under the above assumptions, the counting process is a submartingale. Hence, according to the Doob-Meyer decomposition theorem, it can be decomposed as follows:

$$N_{sr}(t) = \Lambda_{sr}(t) + M_{sr}(t),$$

where $\Lambda_{sr}(t) = \int_0^t \lambda_{sr}(\tau) d\tau$ represents the predictable part of the counting process and $M_{sr}(t)$ is a zero-mean martingale. From a structural point of view, the generative process Λ only depends on \mathbf{X}_{PA} , where causal parents set $PA \subset \{1, \dots, p\}$. In Figure 1, the causal parents consist of covariates 2 and 3.

The hazard function $\lambda_{sr}(t)$ represents the rate of the event (s, r) occurring at time t .

Without loss of generality, the hazard rate can be written as

$$\lambda_{sr}(t) = \mathbb{1}_{\{(s,r) \in \mathcal{R}(t)\}} \lambda_0(t) \exp \{f_{PA}(\mathbf{X}_{sr}(t))\}. \quad (1)$$

where the risk set $\mathcal{R}(t)$ is the set of events that are at risk of happening at time t , $\lambda_0(t)$ is the baseline hazard function unrelated to (s, r) and $f_{PA} : \mathbb{R}^p \rightarrow \mathbb{R}$ is the relative risk function depending only on the causal parents. A special case is where the function is linear, i.e., $f_{PA}(x) = \beta_{PA}^t x_{PA}$, where β_{PA} is the linear causal parameter.

The causal parameter solves a population likelihood maximization conditional on the true causal parents. Unfortunately, this property does not help to identify the causal parameters, as the overall maximization will in general identify a function that depends on all the covariates in the Markov blanket of N .

2.2 Invariant causal prediction for dynamic network models

The aim of this section is to define a property that identifies the causal risk function f_{PA} irrespective of knowing the set of causal parents. We will define a partial likelihood for the process N and show that its associated Pearson Risk is exactly 1 for the causal model,

$$R^P(f_{PA}) = 1. \quad (2)$$

Together with population maximum likelihood the Pearson risk invariance property (2) can be shown to uniquely identify the structural relational event model.

Let n be the (random) number of relational events in $[0, T]$, we can define a nested case-control partial likelihood (Borgan et al., 1995; Filippi-Mazzola and Wit, 2024) associated with the dynamic network N as

$$\begin{aligned} \ell(f) &= \log \prod_{i=1}^n \frac{\exp \{f(\mathbf{X}_{s_i r_i}(t_i))\}}{\exp \{f(\mathbf{X}_{s_i r_i}(t_i))\} + \exp \{f(\mathbf{X}_{s_i^* r_i^*}(t_i))\}} \\ &= \log \prod_{i=1}^n \frac{\exp \{f(\mathbf{X}_{s_i r_i}(t_i)) - f(\mathbf{X}_{s_i^* r_i^*}(t_i))\}}{1 + \exp \{f(\mathbf{X}_{s_i r_i}(t_i)) - f(\mathbf{X}_{s_i^* r_i^*}(t_i))\}}, \end{aligned}$$

where at event time t_i of event (s_i, r_i) , a non-event $(s_i^*, r_i^*) \neq (s_i, r_i)$ is randomly sampled from the risk set $\mathcal{R}(t_i)$. The last equality corresponds to the log-likelihood of a degenerate logistic regression model with response $\mathbf{Y} = (1, \dots, 1)$ and non-linear predictor $\Delta_i f = f(\mathbf{x}_{s_i r_i}(t_i)) - f(\mathbf{x}_{s_i^* r_i^*}(t_i))$. As this partial likelihood of N is an exponential dispersion family, Polinelli et al. (2024) show that, at the population level, f_{PA} satisfies the following two conditions, which identify it up to a zero set:

1. f_{PA} maximises the population likelihood of Y and \mathbf{X}_{PA} :

$$f_{PA} = \arg \max_f \mathbb{E}_{\mathbf{X}_{PA}, N} [\ell(f)].$$

2. f_{PA} achieves perfectly dispersed population Pearson risk:

$$\mathbb{E}_{\mathbf{X}, N} \left[\frac{(Y - \dot{b}(\Delta_i f_{PA}))^2}{\ddot{b}(\Delta_i f_{PA})} \right] = a(\phi),$$

where $\dot{b}(\cdot)$ and $\ddot{b}(\cdot)$ are the first and second derivative of the cumulant generator function $b(\cdot)$, respectively.

Using the fact that for a binomial distribution the dispersion parameter $a(\phi) = 1$ and cumulant function $b(\theta) = \log(1 + \exp(\theta))$, we can now define an empirical causal discovery procedure for the causal dynamic network.

2.3 Empirical algorithm for causal discovery in dynamic network model

An empirical version of the causal discovery algorithm can be proposed, when observing a sample $\{(\mathbf{x}_i(t_i), (s_i, r_i), (s_i^*, r_i^*) \mid i = 1, \dots, n\}$ of size n , in which the condition of having a perfectly dispersed Pearson risk is checked via a statistical test. By approximating the non-linear f via a finite basis expansion ψ , the inference can be performed by means of generalized additive models. In particular, let $S \subseteq \{1, \dots, p\}$ a set of potential causal drivers of N . There exist $|S|$ -dimensional basis ψ_S such that $f_S : \mathbb{R}^{|S|} \rightarrow \mathbb{R}$ can be written as $f_S(\mathbf{x}_S) = \boldsymbol{\beta}_S^\top \psi_S(\mathbf{x}_S)$. In the following algorithm, the focus will be on $\boldsymbol{\beta}_S$ rather than f_S .

1. For any set of covariates \mathbf{X}_S , with $S \subset \{1, \dots, p\}$, find the penalised maximum likelihood estimator:

$$\hat{\boldsymbol{\beta}}_S = \arg \max_{\boldsymbol{\beta}} \left[\sum_{i=1}^n (\boldsymbol{\beta}^\top \psi_S(\mathbf{x}_{i,S}) - b(\boldsymbol{\beta}^\top \psi_S(\mathbf{x}_{i,S}))) + P_\lambda(\boldsymbol{\beta}) \right],$$

where $\mathbf{x}_{i,S}$ is the i^{th} realization of \mathbf{X}_S and P_λ is a suitable smoothness penalty function. Furthermore, we used the fact that $y_i = 1$ for all $i = 1, \dots, n$ as we are dealing with a degenerate logistic model.

2. Find $S_1, \dots, S_K \subset \{1, \dots, p\}$ such that

$$H_0 : \mathbb{E}_{\mathbf{X}, Y} \left[\frac{(Y - \dot{b}(\boldsymbol{\beta}_{S_k}^\top \psi_{S_k}(\mathbf{X}_{S_k})))^2}{\ddot{b}(\boldsymbol{\beta}_{S_k}^\top \psi_{S_k}(\mathbf{X}_{S_k}))} \right] = 1$$

cannot be rejected. To this purpose, we use the Pearson risk statistic

$$R(\hat{\boldsymbol{\beta}}_{S_k}) = \sum_{i=1}^n \left[\frac{(1 - \dot{b}(\hat{\boldsymbol{\beta}}_{S_k}^\top \psi_{S_k}(\mathbf{x}_{i,S_k})))^2}{\ddot{b}(\hat{\boldsymbol{\beta}}_{S_k}^\top \psi_{S_k}(\mathbf{x}_{i,S_k}))} \right],$$

in which $\hat{\boldsymbol{\beta}}_{S_k}$ denotes the penalized maximum likelihood estimator. Under the null hypothesis, the Pearson statistics is approximately chi-squared distributed, with $n - |S_k|$ degrees of freedom. Hence, a two-sided statistical test is performed, in order to select perfectly dispersed models. In practice, it has to be checked that

$$\chi_{n-|S_k|, \frac{\alpha}{2}}^2 \leq \sum_{i=1}^n \left[\frac{(1 - \dot{b}(\hat{\boldsymbol{\beta}}_{S_k}^\top \psi_{S_k}(\mathbf{x}_{i,S_k})))^2}{\ddot{b}(\hat{\boldsymbol{\beta}}_{S_k}^\top \psi_{S_k}(\mathbf{x}_{i,S_k}))} \right] \leq \chi_{n-|S_k|, 1-\frac{\alpha}{2}}^2$$

for some significance level α .

3. Among perfectly dispersed models f_{S_1}, \dots, f_{S_K} , i.e., smooth functions associated with $\boldsymbol{\beta}_{S_1}, \dots, \boldsymbol{\beta}_{S_K}$, select the one that minimises BIC as in the population case.

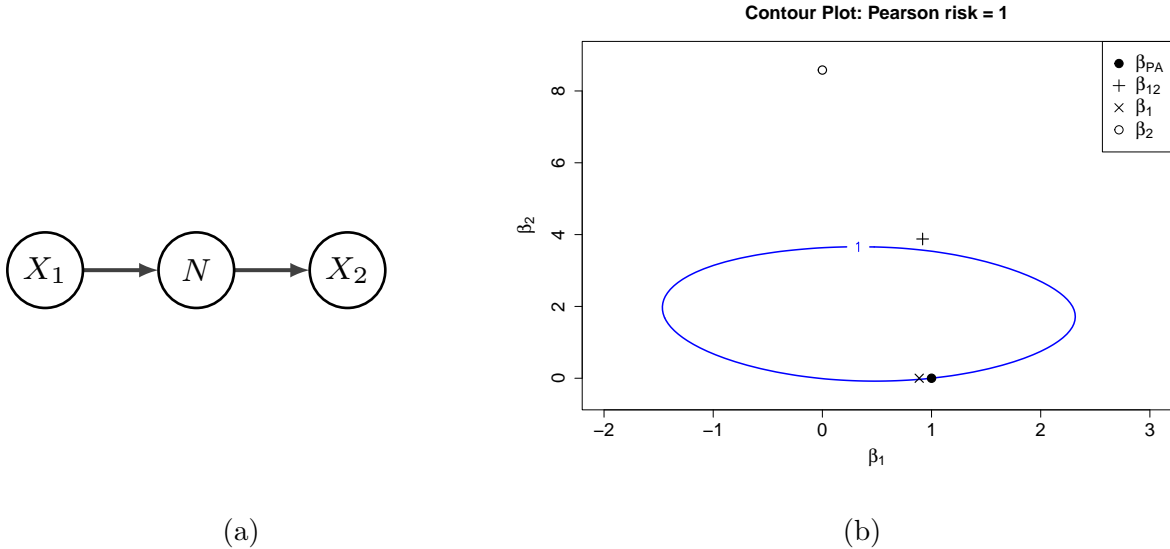


Figure 2: Structural Relational Event Process N with 2 covariates X_1 and X_2 .

2.4 An illustrative example

Let consider the structural relational event model in Figure 2a. In this system, X_1 is a parent of the relational process N , whereas X_2 is its child. Hence, the generative hazard rate depends only on the first covariate. In particular, the following hazard rate has been chosen to generate data:

$$\lambda_{sr}(t) = \mathbb{1}_{\{(s,r) \in \mathcal{R}(t)\}} \exp \{ \mathbf{x}_{sr,1}(t) \}.$$

Notice that the baseline hazard is assumed to be constant over time. Moreover, the causal parameter vector is $\boldsymbol{\beta}_{PA} = (1, 0)$.

In a structural relational event model with two covariates, there are three possible models to consider: (i) X_1 is causal parent (true model), (ii) X_2 is causal parent, or (iii) both X_1 and X_2 are causal parents. Figure 2b shows the contour line of Pearson risk equal to 1. This clearly shows that Pearson risk invariance alone is not sufficient to identify the causal model. Furthermore, the log-likelihood function has been maximised for all the three possible models: β_{12} is the MLE of the full model, β_1 is the MLE of the model with only X_1 and β_2 is the MLE of the model with only X_2 . The estimates are indicated by various symbols. It is clear that only β_1 lies near the contour line of the perfectly dispersed Pearson risk, close to the true causal parameter, thereby correctly identifying X_1 as the true causal driver. The other MLEs do not satisfy this property.

3 Simulation study

In this section, we show the effectiveness of the proposed approach by means of a simulation study. We consider a causal REM with 7 covariates as in Figure 3a with data distributed according to the linear structural equation model described in 3b.

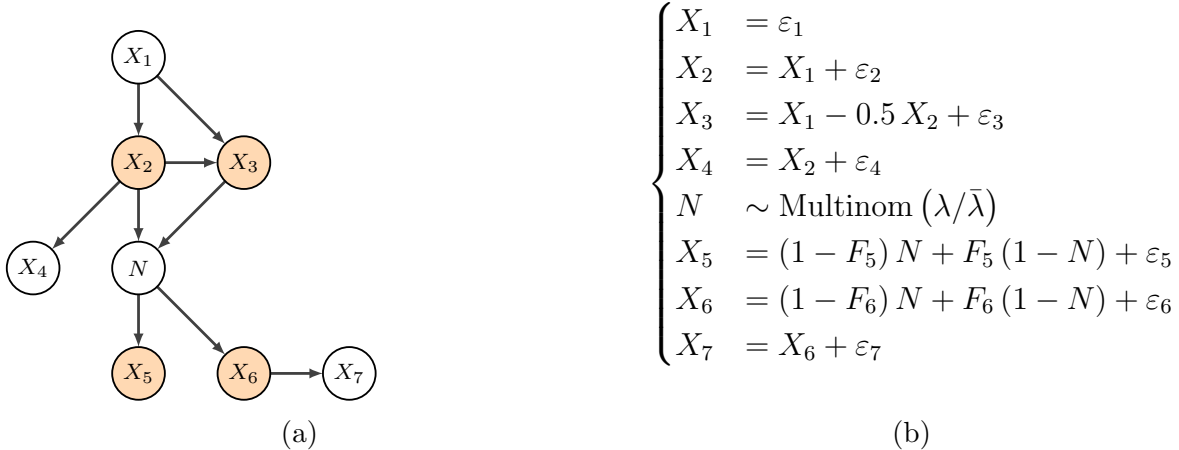


Figure 3: Causal REM with 7 covariates with nodes in orange belonging to the Markov Blanket of the relational process N with hazard rates $\lambda = \{\lambda_{sr}\}_{(s,r) \in V_1 \times V_2}$ and $\bar{\lambda} = \sum_{(s,r) \in \mathcal{R}(t)} \lambda_{sr}(t)$. The causal parents of N are X_2 and X_3 .

The relational process N has two causal parents, X_2 and X_3 . We define the collection of intensity processes λ , with components λ_{sr} as in (1), such that $f_{PA}(x_2, x_3) = 0.8 x_{sr,2}(t) - 0.9 x_{sr,3}(t)$. For simplicity, in this case we assume the baseline hazard to be constant over time. Furthermore we consider $V_1 = V_2 = \{1, \dots, v\}$ and that all the v^2 possible interactions are always at risk of happening. Then, using a Gillespie-type algorithm (Gillespie, 1976), we generate n relational events according to this hazard. The variables ε_i , $i = 1, \dots, 4$, are uniformly distributed over different ranges. N is the multivariate counting process, handled as a matrix of dimensions $v^2 \times n$: for each column, it has an entry equal to 1 corresponding to the occurred event and 0 everywhere else. The children, namely X_5 and X_6 are obtained by flipping some entries in the columns of N through the matrices F_5 and F_6 respectively. Lastly, ε_j for $j = 5, 6, 7$ are normally distributed.

We perform 100 replications with fixed sample size $n = 10^4$. As the causal REM involves 7 covariates, there are $2^7 - 1 = 127$ possible models. Since only linear fixed effects are assumed in this setting, each model is fitted using the R function `glm`. The Pearson risk is computed using the estimated parameters.

Is the true causal model predictive? Figure 4a shows the boxplot of the BIC values of all the models across all the simulations: models are sorted in decreasing order according to the median of the BIC. In a purely predictive context, BIC is often used for model selection, where models with lower BIC are preferred. As expected, the true causal model (red line) is not optimal in a predictive sense having a considerably high BIC compared to other sub-models. In principle, we would expect the model with nodes belonging to the Markov Blanket of N to be the most predictive and indeed in this case, the model with the lowest BIC is the one that includes only the children of the relational process, namely X_5 and X_6 .

Which models have perfectly dispersed Pearson risk? Figure 4b shows the boxplot of the empirical Pearson risk for each model across all the simulations. Also in this case, values are sorted in decreasing order according to their median. The causal model (red line) has perfectly dispersed Pearson risk, but it is not the only one to satisfy this

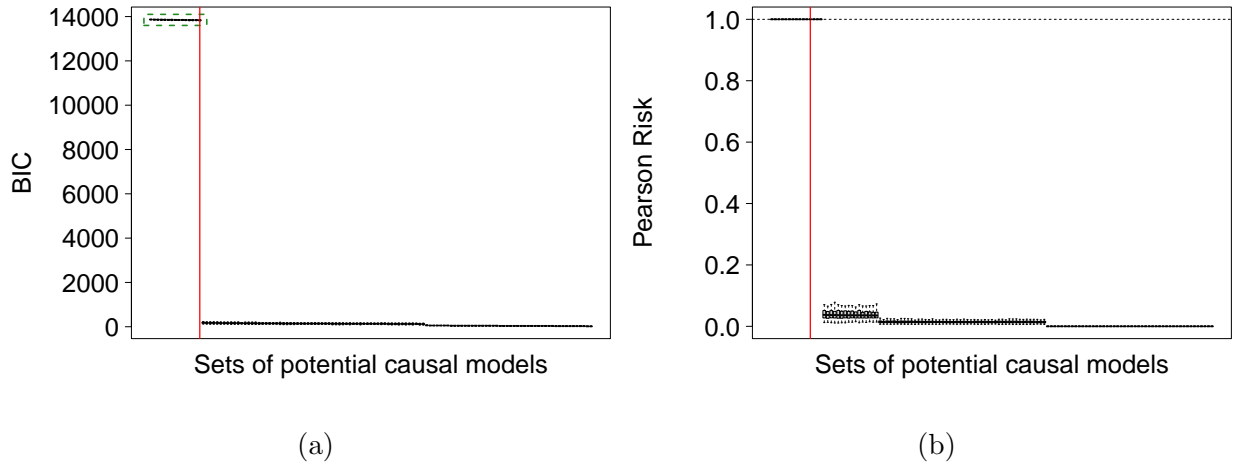


Figure 4: Results across 100 simulations. (a) The causal model (red line) is not the one that minimises BIC, but it is the one with smallest BIC among models with Pearson risk close to 1. (b) The causal model (red line) has perfectly dispersed Pearson risk.

condition. Indeed, all the models containing X_1 , X_2 , X_3 and X_4 also have Pearson risk close to 1. Apart from the true causal parents, variables involved are either ancestors, like X_1 , or variables blocked by causal parents, such as X_4 . Since variables that are d-separated from N in the causal graph by the causal parents are not predictive, models that contain these covariates will have greater BIC among the ones with Pearson risk close to 1. Therefore, the causal model is properly detected as the one with the lowest BIC among those with perfectly dispersed Pearson risk.

How often is the causal model recovered? Figure 5a exhibits all the models found by the RCD, each one with its percentage of detection, using an $\alpha = 5\%$ significance level. The true causal drivers are obtained 81 times over 100 simulations.

Does the sample size have an effect on the detection of the true causal model? As reported in Figure 5b, the efficacy of the approach in recovering the true causal model clearly increases with the sample size n .

4 Causal drivers of bike sharing

In this section we provide an empirical example of the applicability of our method. We will consider a study described in Lembo et al. (2024), which models bike sharing in Washington DC as a relational event process and investigates the effect of a variety of both global and node/edge-specific covariates. This phenomenon, clearly temporal in nature, can be represented via a dynamic network: a sequence of relational events, i.e., bike rides, between a set of vertices, i.e., bike stations, evolving over time.

The data, from the bike sharing provider in Washington DC, Capital Bikeshare (<https://capitalbikeshare.com/system-data>), is publicly available and includes time-stamped and geo-located information on bike rides in the service area. In particular, we will consider a subset of 20,000 randomly sampled events of the dataset analyzed in that paper, which considers bike shares during the period July 9th-31st, 2023. An interaction is observed from a station s to another station r at time t if a bike is taken from station s at time t

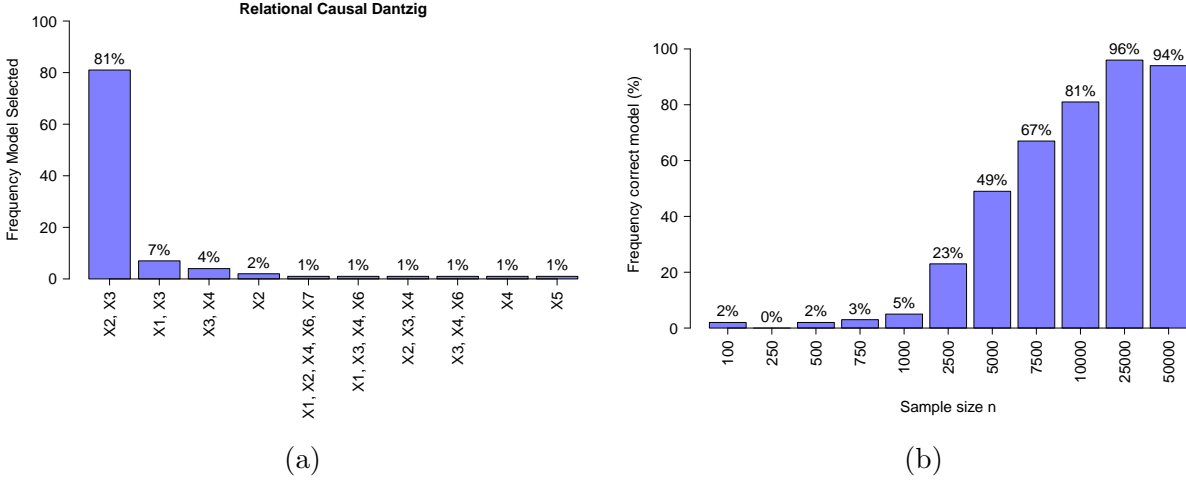


Figure 5: Results across 100 simulations (a) The true causal model is selected 81% of the times for $n = 10,000$. (b) The larger the sample size, the better causal discovery becomes.

and is then left at station r some time after. As a result of the instantaneous nature of the events assumed in REMs, duration of the ride is ignored. We consider the following potential causal drivers of bike sharing:

- **Global covariates** model the role weather plays in describing this phenomena by accounting for temperature (measured in $^{\circ}\text{C}$) and precipitation (measured in mm and log-transformed). They also account for intrinsic temporal effects like a global time effect, and a covariate for time-of-day.
- **Node-level covariates** capture any sender/receiver bike station competition effect related to their geographical position.
- **Dyadic covariates** account for the distance between stations and endogenous effects of repetition, i.e., tendency to repeat the same route over time, and reciprocity, capturing the propensity to bike in along a specific route having previously bike along the same route but in the opposite direction.

We fit every possible sub-model (in total 511 of them, excluding the empty one) according to method proposed in Lembo et al. (2024), that extends the nested case-control partial likelihood approach, mentioned in Section 2.2, to the case in which global covariates are of interest and also included in the hazard. We then employ the empirical algorithm described in Section 2.3 to recover causal drivers. Applying the invariant prediction procedure, results in a causal model that involves the following covariates: time of the day, sender station competition, reciprocity and repetition. Figure 6a shows the plot of the BIC values for each of the fitted models. The causal one (red line) is far from being the most predictive. Indeed, the model with the lowest BIC includes time of the day, sender station competition, receiver station competition, distance among stations, repetition and reciprocity. Figure 6b instead shows the base 10 logarithm of the Pearson risk: the causal model is the one with the lowest BIC among those with perfectly dispersed Pearson risk.

Having detected the causal drivers, we can analyze the estimated effects of these variables. Figure 7 shows how time of the day influences the volume of bike shares. During

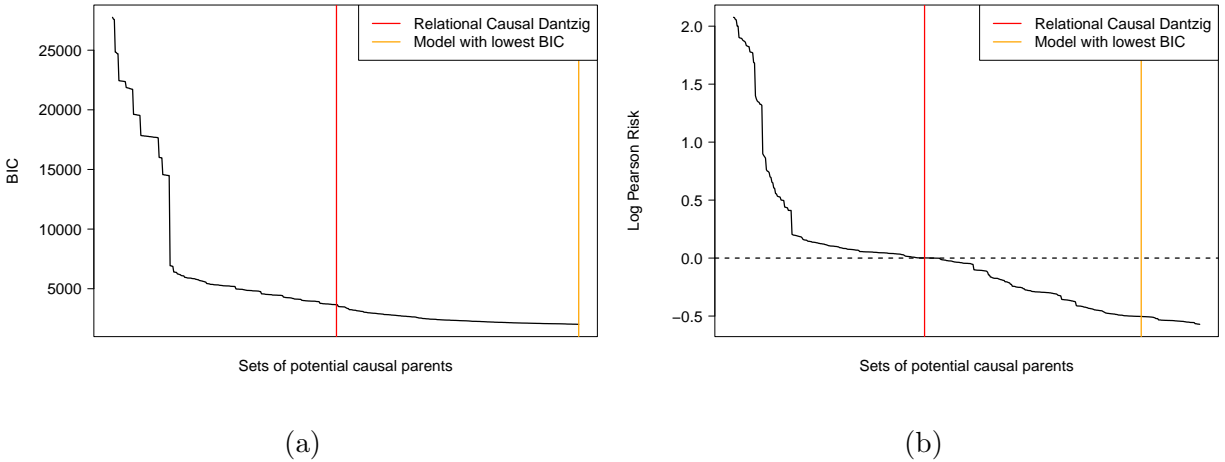


Figure 6: (a) BIC values and (b) base 10 logarithm of Pearson risk values for all models fitted on the analyzed bike sharing data. The causal model (red line) is far from being the most predictive, since it has a high BIC value but it has perfectly dispersed Pearson risk.

the night, there is a huge decline, in contrast with what happens during the day. More specifically, the plot presents two peaks at 9 a.m. and at 6 p.m., that is when workers commute to and from workplaces. Interestingly, the intensity of bike sharing is greater in the late afternoon than the peak observed in the morning.

From Figure 8a, it can be noted that there is a daily trend in the bike sharing. The peak at 24 hours suggests that the same route is traveled with a daily frequency. Lastly, Figure 8b reveals that, given a specific route, the tendency to observe the opposite one overall generally decreases as time passes. The peak after 12 hours could correspond to the moment in which a day work ends and people taking the same route they previously did, but in the opposite direction.

Related to the start competition, the estimated linear fixed effect is negative, equal to -0.41270 (SE 0.0273 , p -value < 0.0001). Interestingly, this means that there is a “negative competition” scenario. Indeed, the variable is defined in terms of the distance between the starting station and its closest bike station, measured in biking minutes. So, the smaller the value of the variable, the higher the competition. Thus, a negative value of the parameter could suggest that the number of stations and their placement are not enough to sustain the high demand of bike shares in the area.

5 Conclusions

In conclusion, this study has presented a novel approach to identifying causal drivers within dynamic network models by extending the relational event framework. Through our proposed model and empirical algorithm, we have demonstrated that invariant causal prediction is feasible with data from a single environment, which significantly enhances practical applicability in fields such as social, financial, and environmental systems. Simulation results have underscored the model’s accuracy in detecting true causal relationships. Applied to the dynamic bike-sharing network, the approach successfully revealed causal factors that align with intuitive temporal and spatial patterns in urban mobility. These findings suggest

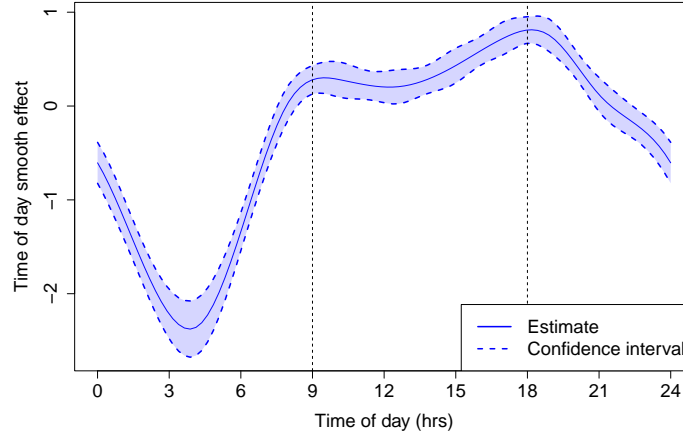


Figure 7: Effect of time of the day on bike sharing. Daylight favors bike routes, with peaks at 9 a.m. and 6 p.m. when people potentially commute to work. At night, the tendency of bike sharing decreases.

that our method provides a robust tool for causal inference in complex, temporal networks, opening avenues for further research and practical applications in data-rich, dynamic environments. Future work could explore extending this methodology to multi-layered networks and adapting it to domains with heterogeneous data structures.

Acknowledgment

This work was supported by funding from the Swiss National Science Foundation (grant 192549).

References

- Angrist, J. D., G. W. Imbens, and D. B. Rubin (1996). Identification of causal effects using instrumental variables. *Journal of the American Statistical Association* 91(434), 444–455.
- Bianchi, F., E. Filippi-Mazzola, A. Lomi, and E. C. Wit (2024). Relational event modeling. *Annual Review of Statistics and Its Application* 11.
- Borgan, Ø., L. Goldstein, and B. Langholz (1995). Methods for the analysis of sampled cohort data in the cox proportional hazards model. *The Annals of Statistics* 23(5), 1749–1778.
- Butts, C. T. (2008). A relational event framework for social action. *Sociological Methodology* 38(1), 155–200.
- Filippi-Mazzola, E. and E. C. Wit (2024). A stochastic gradient relational event additive

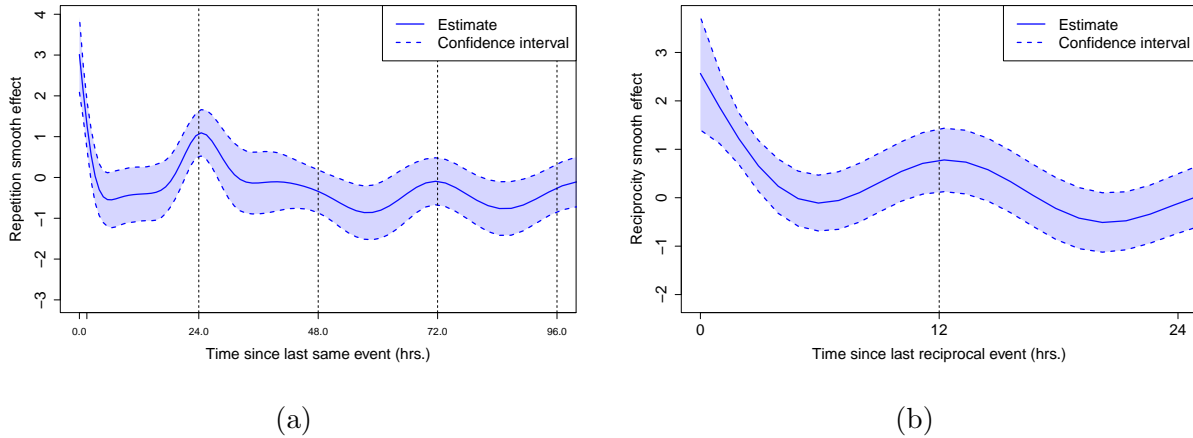


Figure 8: Dyadic endogenous effects on bike sharing: (a) Repetition captures a daily pattern suggesting a tendency to go through the same route every day. (b) Reciprocity overall generally decreases as time passes, but a peak after almost 12 hours can be noticed, potentially related to a return trip in the opposite direction.

model for modelling us patent citations from 1976 to 2022. *Journal of the Royal Statistical Society Series C: Applied Statistics* 73(4), 1008–1024.

Gillespie, D. T. (1976). A general method for numerically simulating the stochastic time evolution of coupled chemical reactions. *Journal of Computational Physics* 22(4), 403–434.

Lembo, M., R. Juozaitienė, V. Vinciotti, and E. C. Wit (2024). Relational event models with global covariates.

Peters, J., P. Bühlmann, and N. Meinshausen (2016). Causal inference by using invariant prediction: Identification and confidence intervals. *Journal of the Royal Statistical Society Series B: Statistical Methodology* 78(5), 947–1012.

Polinelli, A., V. Vinciotti, and E. C. Wit (2024). Generalised causal dantzig.

Rothenhäusler, D., P. Bühlmann, and N. Meinshausen (2019). Causal dantzig: fast inference in linear structural equation models with hidden variables under additive interventions. *The Annals of Statistics* 47(3).

Spirites, P. and C. Glymour (1991). An algorithm for fast recovery of sparse causal graphs. *Social Science Computer Review - SOC SCI COMPUT REV* 9, 62–72.